buildings

MDPI

Article

Research on Rural Landscape Emotions Based on EEG Technology and VIKOR-GRA Model: A Case Study of Xiedian Ancient Village in Macheng City

Xinyu Yan and Yifei Li *

School of Art & Design, Wuhan University of Science and Technology, Wuhan 430065, China; 202319703004@wust.edu.cn

* Correspondence: liyifei@wust.edu.cn

Abstract

This study integrates EEG technology with the VIKOR-GRA model to construct a quantitative method for assessing emotional responses to rural landscapes. Taking 94 scenes from Xiedian Ancient Village in Macheng City, Hubei Province, as the research objects, arousal (Arousal) and valence (Valence) were calculated based on the power ratio of α and β frequency bands. The entropy weight method was employed to determine weights and compute group utility value (*S*), individual regret value (*R*), and compromise solution (*Q*). The results indicate that 16 scenes had *Q* values > 0.75 (Grade IV), reflecting poor emotional experiences, with significantly lower arousal (-2.15 ± 0.38) and valence (-0.87 ± 1.02). Vegetation morphology and water visibility were identified as the primary limiting factors, while graphic symbols and historical culture exhibited strong positive feedback. Optimization strategies are proposed, providing a quantifiable technical pathway for the renewal of rural heritage landscapes.

Keywords: EEG technology; physiological measurement; VIKOR-GRA model; obstacle analysis; landscape emotion; traditional villages

check for updates

Academic Editors: David Arditi and Antonio Formisano

Received: 23 June 2025
Revised: 1 August 2025
Accepted: 22 August 2025
Published: 23 August 2025

Citation: Yan, X.; Li, Y. Research on Rural Landscape Emotions Based on EEG Technology and VIKOR-GRA Model: A Case Study of Xiedian Ancient Village in Macheng City. *Buildings* **2025**, *15*, 3002. https://doi.org/10.3390/buildings15173002

Copyright: © 2025 by the authors. Licensee MDPI, Basel, Switzerland. This article is an open access article distributed under the terms and conditions of the Creative Commons Attribution (CC BY) license (https://creativecommons.org/licenses/by/4.0/).

1. Introduction

The protection and inheritance of traditional village landscapes are of great significance for rural revitalization. In the interdisciplinary field of contemporary village renewal and landscape design, the objective quantification of environmental emotional perception has become a key issue in improving the quality of built environments. Traditional subjective evaluation methods, such as questionnaires and behavioural observation, struggle to capture instantaneous neural responses in human–landscape interactions, while emerging brain science technologies provide a novel research pathway. With the advancement of EEG technology, the "arousal–valence" two-dimensional model can now quantify emotional experiences of landscapes. However, existing research has predominantly focused on urban environments, with insufficient exploration of rural settings [1].

This study integrates EEG neural monitoring with the VIKOR-GRA decision model. On one hand, it precisely quantifies emotional arousal and valence through the power ratio of α and β frequency bands, overcoming the time-lag limitations of traditional scale methods [2]. On the other hand, it introduces grey relational analysis (GRA) to process the nonlinear characteristics of EEG signals and combines it with the VIKOR algorithm to achieve quantitative assessment of multi-factor synergistic effects. Taking Xiedian Ancient

Village in Macheng, Hubei Province, as the research subject, the study identifies emotional states based on the power of α and β frequency bands in EEG signals and constructs an algorithmic mapping relationship between landscape elements and emotional responses. Through an obstacle degree model, key influencing factors are screened from 94 scenes, providing a quantifiable design basis for village renewal.

2. Research Progress

Electroencephalography (EEG) technology has become an important means of quantifying landscape emotions using physiological indicators due to its high temporal resolution and non-invasive nature. Additionally, this study introduces the VIKOR method and Grey Relational Analysis (GRA), whose data-processing advantages can effectively match the characteristics of EEG signals.

2.1. EEG Acquisition and Analysis

EEG is a bioelectrical signal reflecting the activity of brain neurons. Research shows that modern EEG devices can detect brainwaves across multiple frequency bands, including $\delta, \theta, \alpha, \beta$, and γ, among which β and α waves are often used as indicators to assess environmental adaptability. For example, Boveil utilized β and α waves to analyze the attractiveness of public spaces, finding that the degree of landscape fragmentation influences evaluations of visual and architectural density. Chen Z conducted multi-scenario EEG experiments to compare psychological responses in urban versus natural environments, establishing a relevant experimental research framework [3]. In terms of combining EEG with models, the Lamy team applied it to landscape quality assessment [4].

Recent studies have made significant advances in EEG-based environmental perception research. Pascucci et al. proposed future directions for α-wave studies [5], while Chen et al. enhanced EEG-based emotion recognition accuracy using CNN and GAN deep learning techniques [6]. Alonso-Valerdi et al. opened simulated EEG datasets of the Etzna archeological site to facilitate neuroaesthetic research [7]. Jing et al. developed EEG-based design preference prediction models [8], and Zhang et al. identified that medium window proportions and low-saturation colours best promote relaxation [9]. Zhao et al. EEG data redefines human-centred design [10]. Wang et al. optimized emotional responses through 700-lux rectangular lighting schemes [11].

Karaca et al. employed VR-EEG to reveal correlations between enclosure and coherence in campus landscapes [12], whereas Qin et al. pioneered Transformer-based EEG decoding for 3D gaze-tracking in VR environments [13]. Tiwari et al. established a standardized visual evoked potential dataset from 32 participants to support image classification and brain–computer interface development [14]. Farhangi et al.'s geotagged image analysis across 39 Iranian cities demonstrated that HSV colour features outperform physical structures in predicting attentional states [15].

Xiao et al. determined that 51% green visibility optimizes emotional states via β/α EEG metrics, with building visibility at 5.2% maximizing alertness [16]. Olszewska-Guizzo et al. found stronger frontal α-asymmetry in park versus urban scenes [17]. Rieiro et al. validated NeuroSky (NeuroSky Inc., San Jose, CA, USA) devices' 68% correlation with medical-grade EEG for basic blink detection and resting-state studies [18]. Ren et al.'s decision model highlighted shrubs and tree pits as having the most significant therapeutic effects [19], while Li et al.'s ECG-eye tracking fusion revealed natural riverbanks enhance relaxation whereas artificial elements increase excitement [20].

Current research often focuses on areas such as landscape attention, environmental restorative effects, and visual fatigue, analyzing the correlation between EEG features and landscape quality by comparing typical landscape scenarios. However, EEG-based

landscape quantification research is still in its ear(ly stages, offering significant potential for further exploration.

2.2. VIKOR-GRA Model and Related Research

In the VIKOR-GRA model, the core of VIKOR is to maximize overall benefits while minimizing losses in the worst-case scenario, thereby identifying a compromise solution. GRA, on the other hand, excels at analyzing complex nonlinear relationships in samples under incomplete or uncertain conditions without requiring specific data distributions, making it more effective in handling the random fluctuations of EEG signals [21]. Combining the two methods allows for first determining the relational degree between elements and then making optimal compromise decisions based on this analysis. This characteristic makes the model suitable for scenarios with limited sample sizes and high-dimensional variables. Additionally, the model incorporates an adjustable compromise coefficient to simultaneously maximize group utility (S) and minimize individual regret (R). Taking rural landscape optimization as an example, this model not only enhances overall quality but also effectively avoids elements that may trigger negative emotions.

For instance, Cheng et al. integrated the C-OWA-AHP and VIKOR-GRA methods to optimize the site selection of pumped storage power stations in Anhui, China, identifying Yuexi as the optimal location [22]. Chen et al. developed a VIKOR-GRA-based model to assess flood resilience in Chongqing, filling a gap in the application of the TOSE framework [23]. Wang et al. proposed a six-factor model (including cultural characteristics) based on principal component regression, combined with Kriging interpolation to generate GIS heatmaps of street-level attention distribution [24].

Zhang et al. employed intuitionistic fuzzy DEMATEL-entropy weight method to determine that human factors dominate subway emergency evacuation assessments [25]. Awasthi developed a fuzzy multi-criteria hybrid model (TOPSIS/VIKOR/GRA) for linguistic fuzzy scoring decisions in Luxembourg's tram, bus optimization, and electric vehicle sharing projects [26]. Olabanji et al. combined fuzzy AHP with grey relational matrices to evaluate pipe bending machine design stability, validating robustness through α-coefficient sensitivity analysis [27].

Qi et al. innovatively incorporated D-number reliability indicators using the ID-VIKOR method [28], while also proposing four categories of ideal solution definition rules: benefit-type, cost-type, major qualitative, and minor qualitative criteria [29]. Lu et al. demonstrated through VIKOR-based multi-objective optimization that low-emissivity roof coatings in Chongqing outperform wall insulation in terms of energy-saving benefits [30].

In this study, the process is divided into four parts:

1. Conducting EEG experiments to obtain arousal and valence data and constructing a decision matrix.
2. Using GRA to quantify the relational degree between elements.
3. Generating scenario rankings and emotion levels based on the VIKOR model.
4. Analyzing key constraining factors through an obstacle degree model to provide a "computable" renewal pathway for rural landscapes.

3. Research Subject

Xiedian Ancient Village (originally named Xiedianhe Village) is in Songbu Town, Macheng City, Hubei Province. It was listed in the Catalog of Traditional Chinese Villages in 2016, covering a total area of approximately 15 square kilometres. Situated in the hilly terrain at the southern foot of the Dabie Mountains, the village is bordered by Hongshan Peak to the north and Weidou Lake to the south, with a 3.5 km shoreline. A river runs through its central area, forming a complete ecological structure, as Figure 1.



Figure 1. Aerial and panoramic views of the site (partial).

According to statistical data, the village has a permanent population of 1263, with 28% aged over 60, indicating a pronounced ageing trend. In terms of transportation, the village is approximately 20 kilometres from both Macheng City and Hong'an County. Regarding architectural heritage, the village preserves 42 traditional buildings, predominantly featuring gable (hard hill) and overhanging (hanging hill) roof styles. Historical relics include a stone arch bridge from the Qing Dynasty, a dry-stacked stone wall, and three ancient trees over a century old. On the intangible cultural side, the village follows a single-surname clan settlement pattern, with 82% of villagers sharing the surname, Xie. Their ancestors migrated from Jiangxi during the Hongwu reign of the Ming Dynasty, giving rise to unique cultural traditions such as "Homesick Drumming" and the craftsmanship of layered-cloth shoes (Qiancengdi cloth shoes).

Additionally, the village exhibits distinct spatial characteristics. Its landscape can be categorized into three types: waterfront open spaces, farmland transitional spaces, and building-dense spaces. Field measurements reveal gradient differences in visual complexity (VCI) among these spaces: building-dense spaces: VCI = 3.2 $\pm$ 0.4, farmland transitional spaces: VCI = 2.1 $\pm$ 0.3 and waterfront open spaces: VCI = 1.8 $\pm$ 0.2. This spatial gradient provides an ideal experimental condition for the study.

Despite certain standard deviations in VCI, it was selected as the core classification indicator based on the following empirical findings: Preliminary Pearson correlation analysis revealed that VCI demonstrated stronger correlations with EEG-based emotional responses compared to other candidate indicators. ANOVA tests confirmed statistically significant differences in VCI across three spatial types ($p < 0.05$). When incorporating covariates, including spatial typology and vegetation density, the explanatory power of VCI increased to 82%. Four representative scenes were selected through stratified random sampling, encompassing all three spatial types to ensure comprehensive coverage of environmental element combinations.

4. Research Methodology

Based on the characteristics of rural landscapes and EEG experimental requirements, this study established a three-level observation system comprising 10 dimensions, as Table 1 and Figure 2. The "Material Element Layer" includes built structures (A1), architectural

form (A2), paving materials (A3), and vegetation composition (A4); the "Spatial Perception Layer" covers spatial scale (B1) and visual corridors (B2); while the "Cultural Cognition Layer" involves colour (C1), symbolism (C2), and archetypes (C3). A total of 20 observation indicators were selected, such as "texture of building facades", "patterns of paving combinations", and "hierarchy of plant arrangements" [31].

Table 1. EEG observation element index system.

Category	Element Dimension	Observation Element	Element Description	Element Type and Thresholds		
Material Elements A	Built Structures A1	Landscape Facility Combination A11	Number of facility types	1	2	>2
		Fence Type A12	Fence configuration	Conventional	Graphic	Landscape facility
	Architectural Form A2	Building Combination A21	Number of building types	1	2	>2
		Facade Texture A22	Building facade material type	Stone	Wood	Bamboo
	Paving Materials A3	Paving Material A31	Hard surface material type	Brick	Wood	Concrete
		Paving Combination A32	Number of paving types	1	2	>2
		Paving Condition A33	Paving wear rate	(0, 25]	(25, 50]	>50
	Vegetation Composition A4	Vegetation Morphology A41	Plant configuration	Formal	Semi-natural	Natural
		Vegetation Pattern A42	Planting method	Group planting	Solitary planting	Row planting
		Plant Layers A43	Number of vegetation layers	1	2	>2
	Water Features A5	Water Type A51	Type of water body	River	Well	Other
Spatial Perception B	Spatial Type B1	Spatial Type B11	Spatial representation type	Point	Line	Plane
		Enclosure Degree B12	Proportion of enclosed space	(0, 25]	(25, 50]	>50
	Visual Perception B2	Green View Index B21	Proportion of green plants	(10, 20]	(20, 30]	>30
		Spatial Visibility B22	Spatial depth	Foreground	Midground	Background
Cultural Cognition C	Colour C1	Saturation C11	Colour saturation	(0, 25]	(25, 50]	>50
	Symbol C2	Graphic Symbol C21	Type of graphic symbol	Logo	Signage	Relief
		Symbol Combination C22	Number of symbol types	1	2	>2
	Archetype C3	Text Archetype C31	Type of text identifier	Naming	Decorative	Other
		Historical Culture C32	Era of scene construction	Contemporary	Modern	Ancient

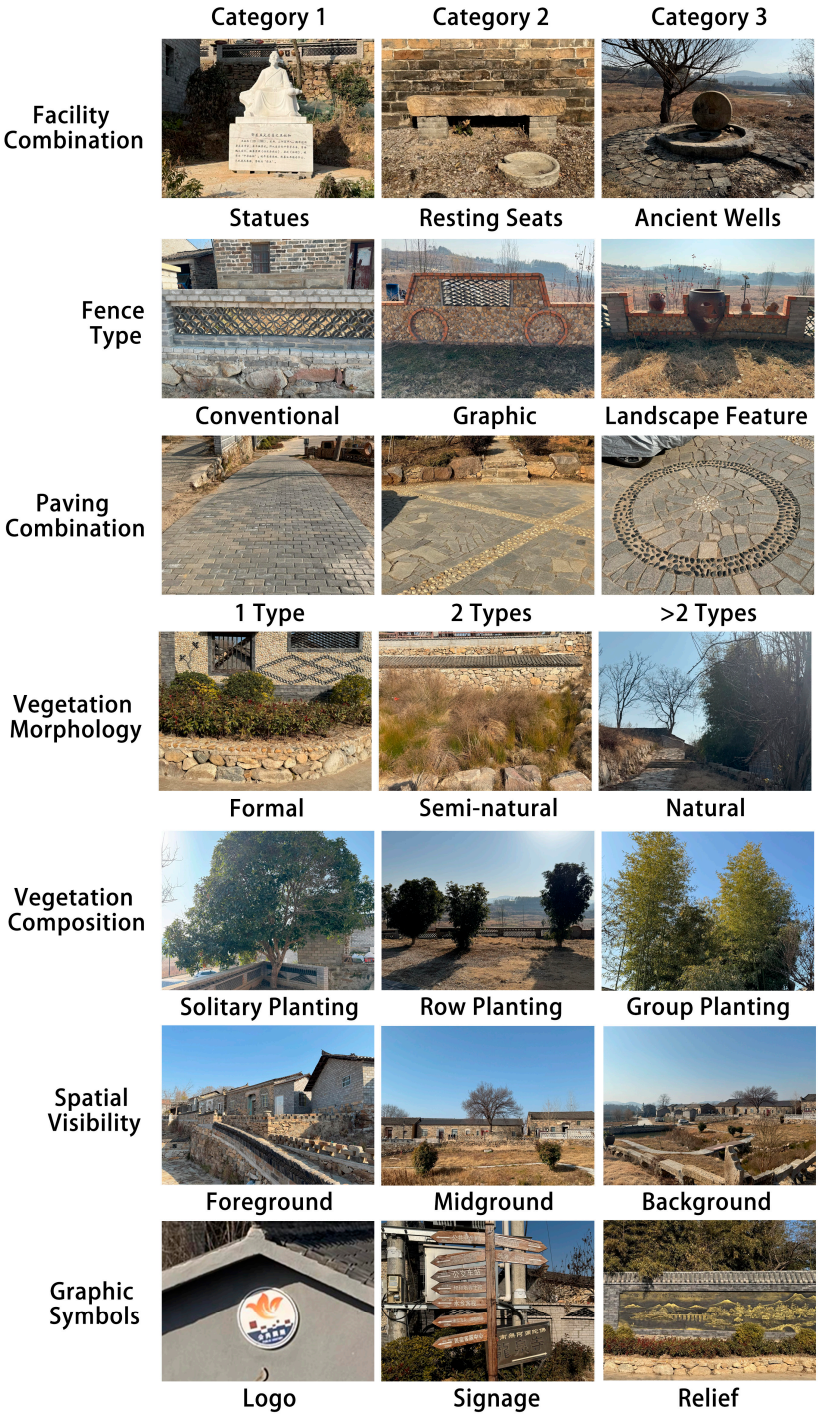

Figure 2. Examples of observation elements (partial).

The threshold values for key variables, including pavement wear rate, were determined based on China's national standard "Assessment Standard for Green Buildings" (GB/T 50378-2019) issued by the Ministry of Housing and Urban-Rural Development, combined with field investigations of 15 comparable traditional villages [32]. The study revealed that when pavement wear exceeds 50%, it causes significant damage to visual coherence, leading to noticeable reductions in surface flatness and a 37% decrease in visual recognizability. More importantly, pre-study questionnaire data demonstrated this level of wear corresponds to a 2.3-fold increase in negative emotional responses, establishing this threshold as a critical design parameter for heritage landscape preservation.

4.1. Data Acquisition

The experiment recruited 30 volunteers (14 male and 16 female) with a mean age of 24.3 ± 2.1 years, all undergraduate or graduate students possessing normal or corrected-to-normal vision who signed informed consent forms [33]. EEG data were collected using a TGAM portable EEG module with a 512 Hz sampling rate and 115,200 baud rate, with stimulus materials derived from 93 standardized landscape scenes from Xiedian Ancient Village processed through Photoshop for uniform white balance and semantic segmentation. The experimental protocol consisted of the following: fixation point (500 ms), emotion test (60,000 ms), stable EEG test (90,000 ms), and scene image presentation (3000 ms), with each scene repeated 3 times and all data collected via *RealTerm (v 2.0.0.70)* serial port [34]. The extended durations for emotion testing and stable EEG measurement accounted for delayed emotional responses observed in rural landscape environments, with the prolonged testing period designed to capture both immediate emotional reactions and sustained cognitive processes—a scheme validated through pre-tests with 15 participants showing EEG patterns stabilizing after 45,000 ms.

A 10 min baseline recording preceded formal testing, with 30 s resting-state recordings inserted after every 5 scenes as local benchmarks, applying linear interpolation algorithms for trend correction during interim periods before final artefact removal of ocular and EMG noise through independent component analysis. The study employed a double-blind controlled design where experimenters were excluded from subsequent data analysis while participants remained unaware of specific scene classifications, maintaining data quality without compromising efficiency.

The study employed the power ratio between α (8–12 Hz) and β (13–28 Hz) frequency bands for quantification, where increased β waves typically indicate higher cognitive load while α waves are associated with relaxed states. This method effectively eliminates the influence of EEG power variations and equipment sensitivity on the research. Here, arousal refers to the intensity of an individual's physiological response to stimuli, reflecting emotional activation levels, while valence represents the positive/negative direction of emotion, i.e., pleasure degree [35] (Equations (1) and (2)):

$$E_{VA} = \frac{P(\alpha)_{right}}{P(\beta)_{right}} - \frac{P(\alpha)_{left}}{P(\beta)_{left}} \tag{1}$$

$$E_{AR} = \frac{P(\alpha)}{P(\beta)} \tag{2}$$

In the equations: E_{VA} denotes valence level, E_{AR} represents arousal level, with value ranges of $[-5, 5]$ where higher absolute values indicate stronger levels; $P(\alpha)$ and $P(\beta)$ refer to the power in α and β frequency bands, respectively.

4.2. VIKOR-GRA Model

The VIKOR-GRA decision algorithm consists of five key components: data normalization, grey relational coefficients, group utility and individual regret, compromise solution (Q value), and obstacle degree analysis:

1. Data Normalization: The α and β power values collected via EEG are normalized using the range method, mapping arousal and valence to the [0, 1] interval. This step eliminates unit differences, enabling cross-comparison of physiological indicators.
2. Grey Relational Analysis (GRA): The optimal reference sequence (e.g., maximum α power) is first determined, followed by calculating the grey relational coefficient for each scenario against this reference. A distinguishing coefficient (ρ = 0.5) balances dif-

ferentiation and noise suppression. The resulting grey relational degree (Γ) quantifies each scenario's proximity to the ideal state.

3. Entropy Weight Determination: The entropy weight method determines weights by calculating the information entropy of indicators, assigning higher weights to low-entropy indicators such as β power with small variation coefficients, while preventing excessive influence from highly variable indicators. Historical–cultural value is quantified through a composite index including construction era (weight 0.4, categorized as contemporary (post–2000), modern (1949–2000), and ancient (pre–1949) based on architectural surveys), cultural symbol density (weight 0.4, measured by counting distinctive cultural elements per 100 m^2), and preservation status (weight 0.2, evaluated through expert scoring), simultaneously considering both temporal and physical attributes.
4. VIKOR Decision Calculation: Group utility (S) measures the weighted deviation across all indicators—lower values indicate better overall performance. Individual regret (R) identifies the worst-performing single indicator, reflecting the "short-board effect." Compromise solution (Q), balances S and R via a coefficient (ν = 0.65), ensuring holistic optimization while mitigating local deficiencies. The Q value categorizes scenarios into four emotional grades.
5. Obstacle Degree Diagnosis: Quantifies the impediment level of each factor to the ideal solution, prioritizing intervention targets for landscape renewal.

4.2.1. Normalization and Grey Relational Coefficient

Due to different dimensions of arousal and valence indicators, normalization methods were employed for data standardization. This step enables a comparison of indicators with different dimensions under the same criteria, effectively preventing extreme indicators from excessively influencing the analysis results. Grey relational analysis enhances the ability to identify subtle differences by introducing the distinguishing coefficient ρ, effectively overcoming data noise interference (Equations (3) and (4)):

$$r_{ij} = \frac{f_{ij} - minf_j}{maxf_j - minf_j} \tag{3}$$

$$\varepsilon_{ij} = \frac{min_i min_j \left| r_j^* - r_{ij} \right| + \rho max_i max_j \left| r_j^* - r_{ij} \right|}{\left| r_j^* - r_{ij} \right| + \rho max_i max_j \left| r_j^* - r_{ij} \right|} \tag{4}$$

In the equations: f_{ij} represents the original value of the j-th indicator for the i-th scene; $maxf_j$ and $minf_j$ denote the maximum and minimum values of indicator j across all scenes, respectively; r_j^* is the positive ideal solution for indicator j; ρ refers to the distinguishing coefficient; the output ε_{ij} ϵ [0, 1], where a larger value indicates a stronger correlation.

4.2.2. VIKOR Multi-Criteria Decision Making

The group utility value S_i reflects the comprehensive performance of scenario i across all evaluation indicators, where a smaller value indicates better overall performance. The individual regret value R_i represents the worst performance of the scenario on a single indicator, with larger values indicating more prominent issues [36]. The Q_i value is adjusted through the decision coefficient v. When v is greater than 0.5, the model places more emphasis on maximizing group benefits, a characteristic particularly suitable for projects that need to balance the needs of the majority (Equations (5)–(7)):

$$S_i = \sum_{j=1}^{n} w_j (1 - \varepsilon_{ij}) \tag{5}$$

$$R_i = max\left[w_j(1-\varepsilon_{ij})\right] \tag{6}$$

$$Q_i = v\frac{S_i - S_{min}}{S_{max} - S_{min}} + (1-v)\frac{R_i - R_{min}}{R_{max} - R_{min}} \tag{7}$$

In the equations: w_j denotes the indicator weight determined by the entropy weight method; v refers to the decision coefficient, emphasizing group utility optimization; S_{min} and S_{max} represent the minimum and maximum values of S_i among the scenarios, respectively.

4.3. Factor Obstruction Model

The factor obstruction model was introduced to conduct correlation analysis on elements affecting emotional quality. It calculates the contribution rate of individual elements to the overall system deviation, clarifies the degree of influence of each indicator, accurately identifies key constraining factors, and formulates optimization strategies accordingly [37] (Equation (8)):

$$Q_j = \frac{(1-\varepsilon_{ij})\cdot W_j^*}{\sum_{j=1}^{n} W_j^* \cdot (1-\varepsilon_{ij})} \tag{8}$$

In the equation: Q_j represents the obstruction degree of observed element j in the scenario, where a larger value indicates stronger constraints; ε_{ij} denotes the grey relational coefficient of element j in scenario i.

5. Analysis of Experimental Results

Through the calculation of group utility value (S), individual regret value (R), and compromise solution (Q), combined with obstruction degree verification, the effectiveness of EEG data in landscape emotional evaluation was confirmed. This section will analyze the results from three perspectives: emotional level distribution, element correlation network, and dominant obstruction factors.

5.1. Landscape Emotional Level Distribution

Based on the VIKOR-GRA model analysis results, the 94 scenes in the study area were divided into four emotional quality levels according to Q values, showing significant uneven spatial distribution characteristics as Table 2 and Figure 3.

Table 2. Statistical distribution of landscape emotion levels (n = 94, age = 24.3 ± 2.1 years).

Grade	Q-Value Range	Number of Scenes	Proportion	Mean Arousal Level	Mean Valence Level	Representative Scene IDs
I	$Q \leq 0.25$	9	9.57%	-0.87 ± 0.28	1.24 ± 0.76	31, 65, 41, 43, 38, 16
II	$0.25 < Q \leq 0.50$	49	52.13%	-1.38 ± 0.41	0.35 ± 0.32	4, 46, 93, 37, 24, 8
III	$0.50 < Q \leq 0.75$	20	21.28%	-1.72 ± 0.38	-0.18 ± 0.45	21, 63, 70, 26, 19, 6
IV	$Q > 0.75$	16	17.02%	-2.15 ± 0.38	-0.87 ± 1.02	60, 72, 17, 52, 91, 94

Among them, 16 Grade IV scenes ($Q > 0.75$) with the worst emotional quality accounted for 17.02% of the total, mainly clustered in the newly built northern area of the village. These scenes showed relatively low emotional response indicators, with an average arousal of -2.15 ± 0.38, significantly lower than the overall level, and a valence value of only 0.13 ± 0.21, indicating emotional suppression. Taking residential structures as an example, obstruction degree analysis revealed that their emotional suppression mainly stemmed from spatial enclosure, possibly due to visual obstruction caused by abandoned equipment.

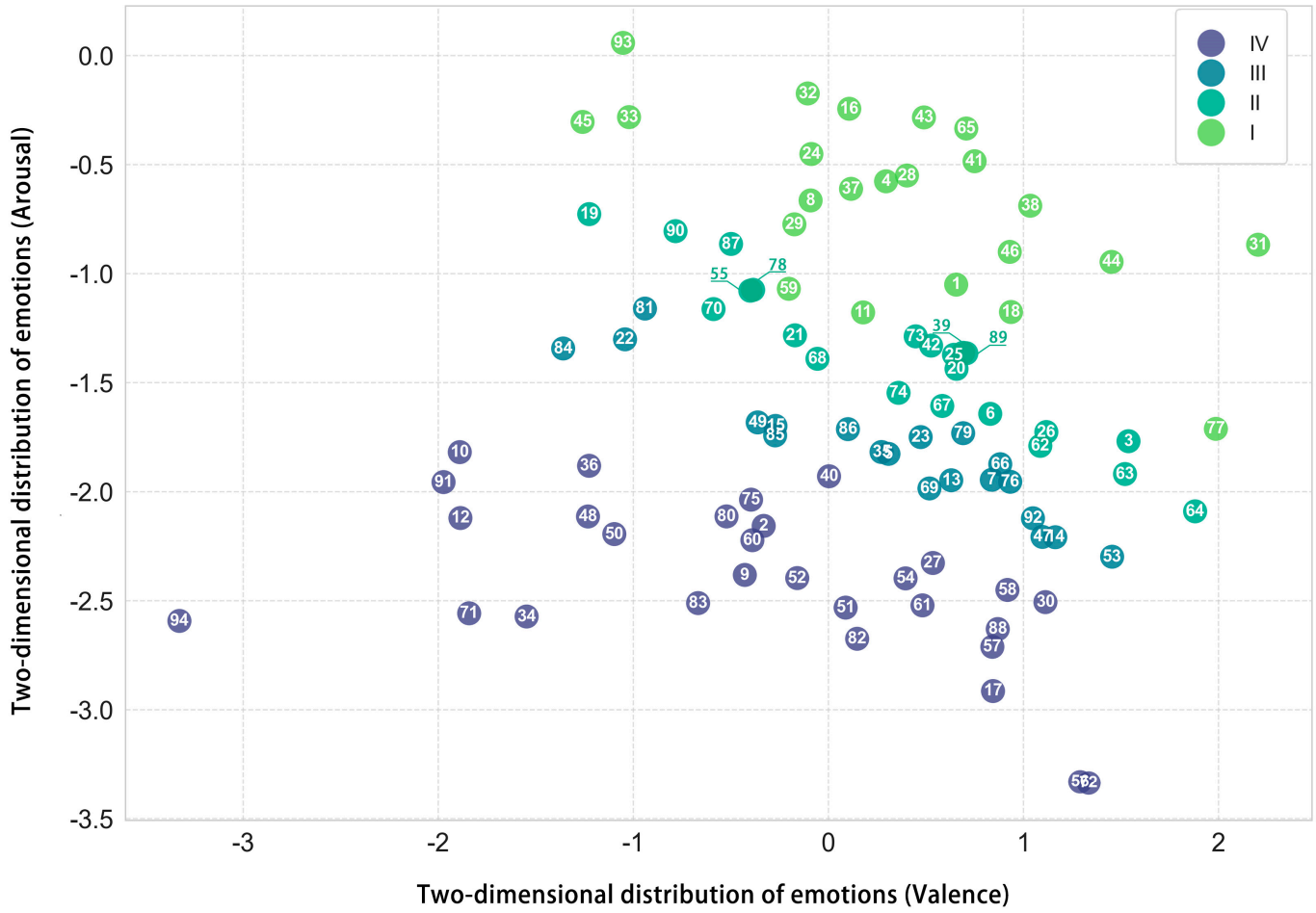

Figure 3. Landscape emotion level distribution map (age = 24.3 ± 2.1 years).

There were 9 Grade I scenes ($Q \leq 0.25$), accounting for 9.57%, primarily concentrated in waterfront areas and historic alleys. Their core characteristics included high water visibility, multi-layered vegetation configuration, and cultural symbol density > 3 features/100 m^2. The square beside newly built homestays emerged as the optimal scene, with a valence value reaching 2.20, where water visibility exceeded 80% and vegetation was arranged in three layers.

5.2. Element Correlation Network Analysis

The grey relational matrix identifies strong correlations when the comprehensive relational degree exceeds 0.75, with this threshold being validated through cluster analysis and conforming to the GRA interpretation standard where r > 0.7 indicates strong relationships, as Figiplier effect, with graphic symbols (C21) and historical culture (C32) forming the strongest positive as Figure 4. Cultural symbols exhibited a multiback loop. In Grade I scenes, these elements synergistically increased valence by 0.35 ± 0.12 (e.g., combining historical slogans with ancient bridges), while their occurrence frequency in Grade IV scenes was only 23% of Grade I levels, reflecting a deficiency in cultural elements.

Vegetation and space demonstrated an antagonistic relationship, where spatial visibility (B22) and vegetation morphology (A41) showed a moderate negative correlation (r = −0.5321). When vegetation density exceeded 70%, spatial visibility obstruction increased to 0.71, leading to a 42% decrease in arousal levels as excessive vegetation coverage induced spatial oppression effects. Paving materials (A31) and spatial types (B11) exhibited strong correlations, with brick paving combined with planar spaces achieving arousal levels

of −0.58, significantly higher than concrete paving scenarios, demonstrating synergistic enhancement effects between paving and space.

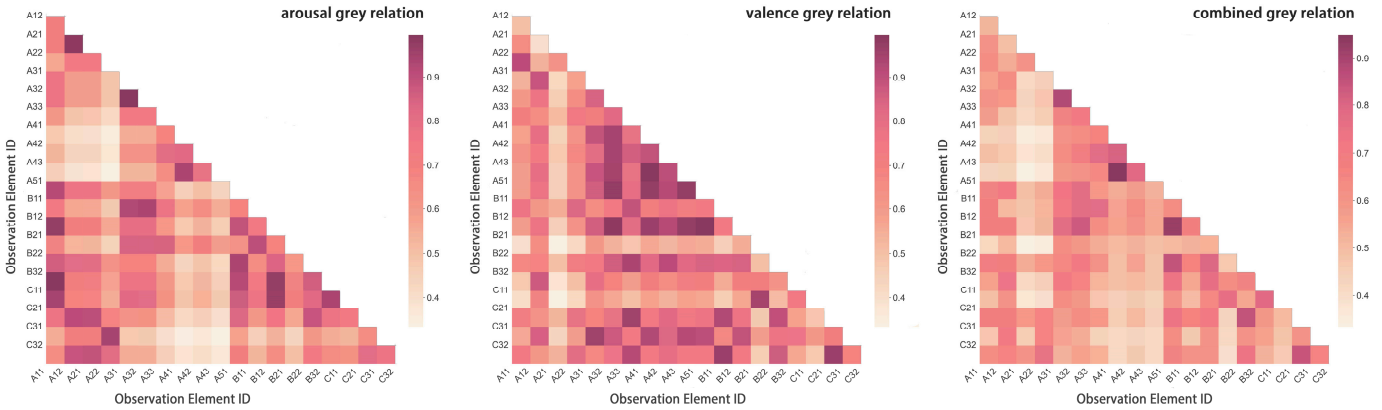

Figure 4. Correlation heatmap of observed elements (age = 24.3 ± 2.1 years; the lower triangular area shows the grey correlation degree between scenarios, where higher values indicate stronger correlations and darker colours represent stronger associations.).

5.3. Dominant Factor Obstruction Diagnosis

The obstruction degree model was employed to quantify element constraint intensity, revealing three typical obstruction patterns as Table 3 and Appendix A**.** The first involves universal obstructions, where water visibility (A51) ranked among the top three across all four grades, showing positive correlation with *Q*-values. When visibility fell below 25%, the probability of *Q*-values rising to 0.58 reached 87%. Vegetation morphology exhibited an average obstruction degree of 0.65, with disordered natural growth resulting in arousal levels 0.95 lower than formal planting arrangements.

Table 3. Distribution of dominant factor obstruction degrees in landscape emotions.

Element Type	Observation Element	Mean Obstruction Degree	Grade Difference	High-Obstruction Scenes	Optimization Priority
Vegetation Composition	A41 Vegetation Morphology	0.65 ± 0.12	+582% ***	30, 47	I
Water Features	A51 Water Visibility	0.68 ± 0.09	+580% ***	66, 5	I
Architectural Form	A21 Building Combination	0.63 ± 0.15	Only in Grade IV *	47	II
Cultural Cognition	C32 Historical Culture	0.29 ± 0.08	−62% **	31, 77	III
Spatial Perception	B22 Spatial Visibility	0.61 ± 0.1	+520% ***	83, 22	I

Notes: The calculation formula for mean obstruction degree refers to Equation (8), "*" indicates $p < 0.05$; "**" indicates $p < 0.01$; "***" indicates $p < 0.001$ (all denote comparisons between Grade IV and Grade I, ANOVA test);Optimization priority follows tiered criteria: Tier I (obstruction degree > 0.6), Tier II (0.4–0.6), and Tier III (<0.4).

The second pattern concerns grade-specific obstructions. Grade IV scenes uniquely showed building composition (A21) obstruction at 0.926, caused by mixing modern materials like concrete with traditional brick–wood structures. In contrast, Grade I scenes demonstrated historical culture obstruction below 0.15, reflecting cultural elements' preservation priority. The third pattern involves synergistic element obstructions. In roadside tree plantings, combined obstructions from vegetation morphology (A41) and spatial visibility

(B22) occurred when canopy coverage exceeded 80%, obscuring cultural symbol recognition and elevating *Q*-values to 0.6818.

6. Design Discussion

The results revealed two key issues affecting emotional quality: inappropriate vegetation configuration and isolated/dispersed cultural elements. In Grade IV scenes, 78% of vegetation showed disordered growth, while canopy coverage exceeding 80% obscured cultural symbol recognition, indicating uncontrolled vegetation morphology weakened cultural visibility. Simultaneously, hierarchical deficiencies were observed—single-layer vegetation scenes accounted for 64% with valence values of only 0.21 ± 0.15, significantly lower than three-layer vegetation scenes, with each additional vegetation layer increasing valence by 0.12. Although text prototypes (C31) and historical culture (C32) showed strong correlation, their average spatial separation reached 45 m (e.g., 62 m between slogan boards and ancestral halls), reducing correlation to 0.58, with spatial dispersion weakening cultural integrity being particularly prominent in redeveloped areas.

Regarding optimization approaches, priority will be given to the renovation of Grade IV scenes through a hierarchical vegetation rehabilitation strategy comprising: 60% formal arrangements (such as Camellia oleifera and Pinus massoniana hedges), 30% mixed configurations (incorporating ancient tree clusters with tree-shrub-herb combinations), and 10% natural conservation areas (e.g., Chinese fir forest reserves).

Specific implementation measures include:

1. Establishing an 800 m formally trimmed Camellia oleifera hedge along the main entrance to the ancient stone arch bridge route, creating a characteristic landscape boundary of eastern Hubei.
2. Developing transitional zones along the Weidou Lake shoreline, centering on three existing century-old trees complemented by Chinese toon (Toona sinensis), ginkgo (Ginkgo biloba) and other arboreal species, integrated with wild chrysanthemum (Chrysanthemum indicum) and other herbaceous plants.
3. Implementing protective measures for native Chinese fir (Cunninghamia lanceolata) forests to maintain natural ecosystems.

Concurrently, cultural corridors will be constructed through installing 2.5-story reliefs per 100 m^2 within the radiation range of ancient city walls and traditional alleys using local bluestone materials, while placing three proverb engravings per 100 m^2 at five key nodal points, including the Nostalgic Drum Performance Square.

The secondary measures focus on enhancing water visibility through graded interventions, including dredging and obstacle removal for three concealed ponds with less than 25% visibility in the northern village area. For irrigation ponds with 25–50% visibility, new viewing platforms constructed from Chinese fir (Cunninghamia lanceolata) will be installed, while maintaining existing conditions for scenes exceeding 50% visibility and simultaneously enriching soundscapes to create audiovisual synergistic effects through coordinated water visibility optimization.

Based on regression models, the implementation of these optimisations is projected to yield a 62% reduction in Grade IV scenes, increase Grade I scenes to 18 (accounting for 19.15% of the total), improve overall valence by 0.41, and enhance cultural perception intensity by 2.3 times. Subsequent phases will incorporate augmented reality (AR) technology to provide real-time optimization prompts and integrate electroencephalogram (EEG) wearable devices to establish closed-loop user emotional feedback systems.

7. Conclusions

This study systematically quantified the spatial differentiation and elemental influences of landscape emotions in Xiedian Ancient Village using the EEG-based VIKOR-GRA model. The results revealed a polarized distribution of landscape emotion grades, with particularly low arousal and valence levels concentrated in the northern newly developed areas. Cross-grade obstruction factors demonstrated significant effects, while the strong positive correlation between graphic symbols and historical culture confirmed notable synergistic effects of cultural elements.

Building on these findings, the study proposed a "vegetation-culture-water" optimization framework. Through vegetation rehabilitation, increased cultural symbol density, and tiered water visibility regulation, the proportion of Grade IV scenes could be reduced and overall valence values improved. After implementation, Grade IV scenes are projected to decrease by 62%, with an overall valence improvement of 0.41. Future research will incorporate multisensory interactions to expand dimensional analysis and broaden the age range of participants to enhance generalizability, ultimately providing quantifiable and replicable design guidelines for rural landscape renewal.

Author Contributions: Conceptualization, X.Y. and Y.L.; methodology, X.Y.; software, X.Y.; validation, X.Y. and Y.L.; formal analysis, X.Y.; investigation, X.Y.; resources, Y.L.; data curation, X.Y.; writing—original draft preparation, X.Y.; writing—review and editing, Y.L. and X.Y.; supervision, Y.L.; project administration, Y.L.; funding acquisition, Y.L. All authors have read and agreed to the published version of the manuscript.

Funding: This research was funded by the Hubei Provincial Social Science Foundation Project (Hubei Provincial Department of Education Philosophy and Social Science Research Major Project), grant number 22ZD040.

Institutional Review Board Statement: Ethical review and approval were waived for this study due to Article 32 of the "Ethical Review Measures for Life Science and Medical Research Involving Humans" (in China), which exempts studies that do not cause harm to individuals, do not involve sensitive personal information or commercial interests, and are conducted through observation without interfering with public behavior, or research using anonymous data.

Informed Consent Statement: Informed consent was obtained from all subjects involved in the study.

Data Availability Statement: The data used to support the findings of this study are included within this article.

Conflicts of Interest: The authors declare no conflicts of interest.

Abbreviations

The following abbreviations are used in this manuscript:

EEG	Electroencephalography
GRA	Grey Relational Analysis
VIKOR	VIseKriterijumska Optimizacija I Kompromisno Resenje

Appendix A

Table A1. IV-tier landscape emotion analysis results.

Scenes	Group Utility Value (S)	Individual Regret Value (R)	Compromise Solution (Q)	Level	Obstruction Degree (Ar)	Obstruction Degree (Va)
40	0.4941	0.2861	0.6692	IV	0.709861	0.290139
30	0.452	0.3192	0.6818	IV	0.943107	0.056893

Table A1. *Cont.*

Scenes	Group Utility Value (S)	Individual Regret Value (R)	Compromise Solution (Q)	Level	Obstruction Degree (Ar)	Obstruction Degree (Va)
58	0.4654	0.3164	0.6939	IV	0.919505	0.080495
27	0.4865	0.3099	0.7086	IV	0.859816	0.140184
75	0.5205	0.293	0.7188	IV	0.660585	0.339415
36	0.5428	0.2829	0.7274	IV	0.489345	0.510655
88	0.478	0.3252	0.729	IV	0.923995	0.076005
54	0.4992	0.3137	0.7334	IV	0.846928	0.153072
2	0.5249	0.3003	0.7398	IV	0.695954	0.304046
80	0.5308	0.2978	0.7424	IV	0.655505	0.344495
10	0.5587	0.2802	0.743	IV	0.386598	0.613402
57	0.4839	0.3289	0.7446	IV	0.925284	0.074716
61	0.5	0.32	0.7475	IV	0.870727	0.129273
60	0.5313	0.3041	0.7564	IV	0.698724	0.301276
72	0.4659	0.3537	0.7723	IV	0.978632	0.021368
17	0.4924	0.3377	0.7742	IV	0.934797	0.065203
52	0.5299	0.3136	0.7742	IV	0.763828	0.236172
91	0.5703	0.2879	0.7746	IV	0.410827	0.589173
56	0.47	0.3535	0.7773	IV	0.97642	0.02358
48	0.5579	0.2978	0.7786	IV	0.545026	0.454974
51	0.5239	0.3205	0.7805	IV	0.818049	0.181951
9	0.5418	0.3128	0.7885	IV	0.720434	0.279566
50	0.558	0.3025	0.7886	IV	0.582653	0.417347
82	0.5274	0.3272	0.7993	IV	0.841199	0.158801
12	0.5783	0.2982	0.8067	IV	0.459741	0.540259
83	0.5586	0.3194	0.8247	IV	0.705883	0.294117
34	0.5926	0.3224	0.8764	IV	0.595926	0.404074
71	0.6006	0.3217	0.8855	IV	0.556298	0.443702
94	0.6364	0.3234	0.9369	IV	0.407826	0.592174

References

1. Ramirez, R.; Palencia-Lefler, M.; Giraldo, S.; Vamvakousis, Z. Musical neurofeedback for treating depression in elderly people. *Front. Neurosci.* **2015**, *9*, 354. [CrossRef] [PubMed]
2. Xu, L.Q.; Meng, R.X.; Chen, Z. Charming streets: The influence of architectural interface and green vision. *Landsc. Gard.* **2017**, *10*, 27–33. [CrossRef]
3. Chen, Z.; He, Y.; Yu, Y. Enhanced functional connectivity properties of human brains during in-situ nature experience. *PeerJ* **2016**, *4*, e2210. [CrossRef] [PubMed]
4. Khushaba, R.N.; Greenacre, L.; Kodagoda, S.; Louviere, J.; Burke, S.; Dissanayake, G. Choice modeling and the brain: A study on the Electroencephalogram (EEG) of preferences. *Expert Syst. Appl.* **2012**, *39*, 12378–12388. [CrossRef]
5. Pascucci, D.; Menétrey, M.Q.; Passarotto, E.; Luo, J.; Paramento, M.; Rubega, M. EEG brain waves and alpha rhythms: Past, current and future direction. *Neurosci. Biobehav. Rev.* **2025**, *176*, 106288. [CrossRef]
6. Chen, J.; Cui, Y.; Wei, C.; Polat, K.; Alenezi, F. Advances in EEG-Based Emotion Recognition: Challenges, Methodologies, and Future Directions. *Appl. Soft Comput.* **2025**, *180*, 113478. [CrossRef]
7. María, A.-V.L.; Pablo, R.-A.J.; José, D.-M.F.; Yareni, P.-C.T.; Guadalupe, V.-R.P.; Sebastián, N.-R.G.; Isaac, I.-Z.D. EEG Data of Museum Visitors Experiencing Visual and Audiovisual Simulations of Edzná, an Archaeological Site in Mexico. *Data Brief* **2025**, *61*, 111855. [CrossRef]
8. Jing, L.; Tian, C.; He, S.; Feng, D.; Jiang, S.; Lu, C. Data-driven implicit design preference prediction model for product concept evaluation via BP neural network and EEG. *Adv. Eng. Inform.* **2023**, *58*, 102213. [CrossRef]
9. Zhang, Z.; Li, Z.; Xu, J. Study on window size and indoor color of typical residential units based on EEG measurement and semantic differential method coupling analysis. *Energy Build.* **2025**, *342*, 115855. [CrossRef]
10. Zhao, M.; Crossley, T.; Shinohara, H. The implications of EEG neurophysiological data in human-centered architectural design: A systematic review and bibliometric analysis. *J. Environ. Psychol.* **2025**, *103*, 102550. [CrossRef]

11. Wang, Y.; Xie, X.; Zhan, X.; Guan, X.; Gou, Z.; Chen, D. Assessing Lighting Layouts in Enclosed Cabins: Multimodal Impacts on Operators and EEG-Based Emotion Modeling. *Build. Environ.* **2025**, *284*, 113444. [CrossRef]
12. Karaca, E.; Çakar, T.; Karaca, M.; Gül, H.H.M. Designing restorative landscapes for students: A Kansei engineering approach enhanced by VR and EEG technologies. *Ain Shams Eng. J.* **2024**, *15*, 102901. [CrossRef]
13. Qin, D.; Long, Y.; Zhang, X.; Zhou, Z.; Jin, Y.; Wang, P. Towards stereoscopic vision: Attention-guided gaze estimation with EEG in 3D space. *Neurocomputing* **2025**, *648*, 130577. [CrossRef]
14. Tiwari, N.; Anwar, S.; Bhattacharjee, V. EEG dataset for natural image recognition through visual stimuli. *Data Brief* **2025**, *60*, 111639. [CrossRef]
15. Farhangi, F.; Sadeghi-Niaraki, A.; Razavi-Termeh, S.V.; Farhangi, F.; Choi, S.-M. Cognitive modeling based on geotagged pictures of urban landscapes using mobile electroencephalogram signals and machine learning models. *Cogn. Syst. Res.* **2025**, *90*, 101324. [CrossRef]
16. Xiao, X.; Li, X.; Zhou, X.; Kang, J.; Luo, J.; Yin, L. Modulatory effects of the landscape sequences on pedestrians emotional states using EEG. *Front. Archit. Res.* **2024**, *13*, 1327–1341. [CrossRef]
17. Olszewska-Guizzo, A.; Sia, A.; Fogel, A.; Ho, R. Can exposure to certain urban green spaces trigger frontal alpha asymmetry in the brain?—Preliminary findings from a passive task EEG study. *Int. J. Environ. Res. Public Health* **2020**, *17*, 394. [CrossRef] [PubMed]
18. Rieiro, H.; Diaz-Piedra, C.; Morales, J.M.; Catena, A.; Romero, S.; Roca-Gonzalez, J.; Fuentes, L.J.; Di Stasi, L.L. Validation of electroencephalographic recordings obtained with a consumer-grade, single dry electrode, low-cost device: A comparative study. *Sensors* **2019**, *19*, 2808. [CrossRef]
19. Ren, H.; Wang, X.; Zhang, J.; Zhang, L.; Wang, Q. Evaluation of Rural Healing Landscape DESIGN Based on Virtual Reality and Electroencephalography. *Buildings* **2024**, *14*, 1560. [CrossRef]
20. Li, M.; Liu, R.; Li, X.; Zhang, S.; Wu, D. The effect of perceived real-scene environment of a river in a high-density urban area on emotions. *Land* **2023**, *13*, 35. [CrossRef]
21. Xiang, Y.; Cao, M. GRA-VIKOR evaluation model for water inrush risk in coastal gold mines based on moment estimation theory. *Min. Res. Dev.* **2025**, *45*, 146–154. [CrossRef]
22. Cheng, X.; Zhao, H.; Zhang, Y.; Hao, X. A study on site selection of pumped storage power plants based on C-OWA-AHP and VIKOR-GRA: A case study in China. *J. Energy Storage* **2023**, *72*, 108623. [CrossRef]
23. Chen, X.; Guo, Z.; Zhou, H.; Qian, X.; Zhang, X. Urban flood resilience assessment based on VIKOR-GRA: A case study in Chongqing, China. *KSCE J. Civ. Eng.* **2022**, *26*, 4178–4194. [CrossRef]
24. Wang, L.; Li, Z.; Zhao, Y.; Ding, H.; Wu, X. Landscape follows attention: Quantitative research on the attention utility of living street scenes based on electroencephalogram rhythms analysis. *Cities* **2025**, *165*, 106135. [CrossRef]
25. Zhang, J.; Huang, D.; You, Q.; Kang, J.; Shi, M.; Lang, X. Evaluation of emergency evacuation capacity of urban metro stations based on combined weights and TOPSIS-GRA method in intuitive fuzzy environment. *Int. J. Disaster Risk Reduct.* **2023**, *95*, 103864. [CrossRef]
26. Awasthi, A.; Omrani, H.; Gerber, P. Investigating ideal-solution based multicriteria decision making techniques for sustainability evaluation of urban mobility projects. *Transp. Res. Part A Policy Pract.* **2018**, *116*, 247–259. [CrossRef]
27. Olabanji, O.M.; Mpofu, K. Appraisal of conceptual designs: Coalescing fuzzy analytic hierarchy process (F-AHP) and fuzzy grey relational analysis (F-GRA). *Results Eng.* **2021**, *9*, 100194. [CrossRef]
28. Qi, J.; Hu, J.; Peng, Y. Interval D-preference-based VIKOR for multiple-criteria group design evaluation with imprecise and unreliable information. *Adv. Eng. Inform.* **2025**, *64*, 103058. [CrossRef]
29. Qi, J.; Hu, J.; Peng, Y. Modified rough VIKOR based design concept evaluation method compatible with objective design and subjective preference factors. *Appl. Soft Comput.* **2021**, *107*, 107414. [CrossRef]
30. Lu, L.; Chen, J.; Liu, Y.; Xu, L.; Ding, Y. Optimizing building energy conservation by balancing energy savings and construction costs of two passive techniques using the VIKOR method: A case study in Chongqing. *J. Build. Eng.* **2025**, *101*, 111885. [CrossRef]
31. Li, Z.; Chen, F.F.; Han, X.; Zhao, K.Y. Quantitative analysis of landscape attention principal components based on electroencephalogram analysis technology—Taking Nanjing Xuanwu Lake Park as an example. *Chin. Gard.* **2021**, *37*, 60–65. [CrossRef]
32. *GB/T 50378-2019*; Announcement on the Partial Revision of the National Standard "Assessment Standard for Green Buildings". Ministry of Housing and Urban-Rural Development: Beijing, China, 2019. Available online: http://www.mohurd.gov.cn/ (accessed on 11 July 2024).
33. Zhang, F.; Hu, M.; Che, W.; Lin, H.; Fang, C. Framework for virtual cognitive experiment in virtual geographic environments. *ISPRS Int. J. Geo-Inf.* **2018**, *7*, 36. [CrossRef]
34. Li, Z.; Wang, L.Y.; Gao, Y.; Li, J. Quantitative study of landscape emotion based on scene electroencephalogram GRA-TOPSIS model—Taking Xiangyang Weidong Factory as an example. *Landsc. Gard.* **2022**, *29*, 33–40. [CrossRef]
35. Zhao, J.; Wu, J.; Wang, H. Characteristics of urban streets in relation to perceived restorativeness. *J. Expo. Sci. Environ. Epidemiol.* **2020**, *30*, 309–319. [CrossRef]

36. Wu, X.S.; Tian, S.X.; Yuan, M.; Ma, R.S.; Lin, H.Y. Research on intelligent evaluation of coal mines based on subjective and objective empowerment VIKOR method. *Min. Res. Dev.* **2021**, *41*, 165–169. [CrossRef]
37. Liu, Q.C.; Han, H.; Li, H.M.; Guo, L. Performance evaluation of sponge city construction based on entropy weight TOPSIS method—Taking Hebi City, Henan Province as an example. *People's Yangtze River* **2017**, *48*, 23–26. [CrossRef]

Disclaimer/Publisher's Note: The statements, opinions and data contained in all publications are solely those of the individual author(s) and contributor(s) and not of MDPI and/or the editor(s). MDPI and/or the editor(s) disclaim responsibility for any injury to people or property resulting from any ideas, methods, instructions or products referred to in the content.